Acta Phys. Hung. A 00/0 (2005) 000–000

HEAVY ION PHYSICS

Primary Cosmic Rays Composition: Simulations and Detector Design

D. Supanitsky[1], G. Medina-Tanco[2], A. Etchegoyen[1], M. Gómez Berisso[3] and C. Medina[1]

[1] Laboratorio Tandar, CNEA
Av. Del Libertador 8250, Buenos Aires, Argentina

[2] Instituto Astronomico e Geofisico, Univ. Sao Paulo
Rua do Matao 1226, Sao Pablo, Brasil

[3] Instituto Balseiro, Centro Atomico Bariloche/CNEA
San Carlos de Bariloche, Argentina

Received 2005

Abstract. The Pierre Auger Observatory is a hybrid detector system for the detection of very high energy cosmic rays. A most difficult and important problem in these studies is the determination of the primary cosmic ray composition for which muon content in air showers appears to be one of the best parameters to discriminate between different composition types.

Although the Pierre Auger surface detectors, which consist of water Cherenkov tanks, are sensitive to muon content they are not able to measure the number of muons directly. In this work we study using simulations the information that can be gained by adding muon detectors to the Auger surface detectors. We consider muon counters with two alternative areas.

Keywords: Ultra-high energy Cosmic Rays, Mass Composition, Muon Detectors
PACS: 96.40.De, 29.40.Mc

1. Introduction

The very nature of the highest energy cosmic rays is far from being understood. Although it is believed that cosmic rays of energies above a few EeV's are mainly of extragalactic origin, there could still be an important contribution of a galactic component to as far as $\sim 10EeV$. The variation of the composition of cosmic

1219-7580/04/ $ 20.00

rays as a function of energy is correlated to their origin. The galactic component gets heavier as energy increases beyond the so-called knee at $10^{15.5}eV$, since only higher charge nuclei may be accelerated at the highest energies by first order Fermi processes operating at supernova remnants. Still, there are experimental evidences which suggest that after $\sim 10^{16.5}eV$ the composition gets lighter again, probably indicating a transition to an incoming extragalactic flux. Between this energy and $\sim 10^{19}$ eV the transition seems to take place. The way in which both components mix inside this energy interval has important implications about the production processes and cosmic magnetic structure both inside the Galaxy and in the intergalactic medium.

It is well known that the number of muons in air showers is very sensitive to primary composition. In particular, showers originated by heavy nuclei produce more muons than lighter ones. The Pierre Auger Observatory is a hybrid detector system which consists of both surface detectors and fluorescence telescopes [1]. The surface detectors are water Cherenkov tanks which are sensitive to air-shower muon contents but they are not able to directly count muons. In Ref. [2] we showed that, among the conventional parameters used in composition studies, the muon number at a certain distance to the shower axis appears to be the best parameter to discriminate proton from iron primaries.

In this work, we use simulations in order to make a comparative study of two possible surface areas for muon detectors. The latter should be added to an infill array embedded inside the Pierre Auger Observatory in order to improve its mass discrimination power.

2. Numerical Methods

2.1. Detector Configuration

The present simulations assume a muon counter array with a grid spacing of $750m$, i.e., half of the present spacing between stations of the Auger surface array. Detectors of two different surface areas, 30 and $60m^2$, were considered. The efficiency of the detectors was assumed as 100%. Each muon counter is placed close to an Auger water Cherenkov tank and buried underground to prevent contamination from shower electrons and gammas (via pair production). The assumed depth was set to have a lower energy threshold of $\sim 0.9GeV$ for a vertical impinging muon, which is equivalent to $1.5m$ of normal rock. Only muons with a higher energy may reach a buried counter since they will loose energy (mainly through ionization) as they propagate downwards through the earth. The energy of a muon that travelled a distance x through the shielding, assuming an energy loss independent of energy and proportional to the track length, is given by:

$$E(x) = E_0 - \alpha \rho x \tag{1}$$

where E_0 is the initial energy, $\rho = 2.65 \times 10^6 gm^{-3}$ the density of the shielding and $\alpha = 2.1 \times 10^{-7} GeV m^2 g^{-1}$ the energy loss per unit column density [3].

2.2. Reconstruction Procedure

We used Aires 2.6.0 [4] with QGSJET01 as the hadronic interaction model in order to simulate extensive air showers. Aires outputs the distribution of particles at the ground level, from which the muon density as a function of the distance to the shower core may be obtained, i.e. the muon Lateral Distribution Function, LDF. We considered the following muon LDF [5],

$$N_\mu(r) = P_0 \left(\frac{r}{r_0}\right)^{-\alpha} \left(1 + \frac{r}{r_0}\right)^{-\beta} \left(1 + \left(\frac{r}{10r_0}\right)^2\right)^{-\gamma} \tag{2}$$

where r is the core distance. We fixed the parameters $r_0 = 320m$ and $\alpha = 0.75$ which led to accurate fits in the energy range of interest, as seen in Fig. 1.

Fig. 1 shows an average Aires simulation of muon LDF's propagated through the rock, for 50 showers of proton and iron of $1.0EeV$ and $30°$ of zenith angle, where the RMS values are within the circles. Also displayed are the fits with the muon LDF of Eq. (2) with $r_0 = 320m$, $\alpha = 0.75$ and P_0, β and γ free fit parameters. It is seen that the LDF parametrization with fixed values of r_0 and α give a quite reasonable fit to the simulated data.

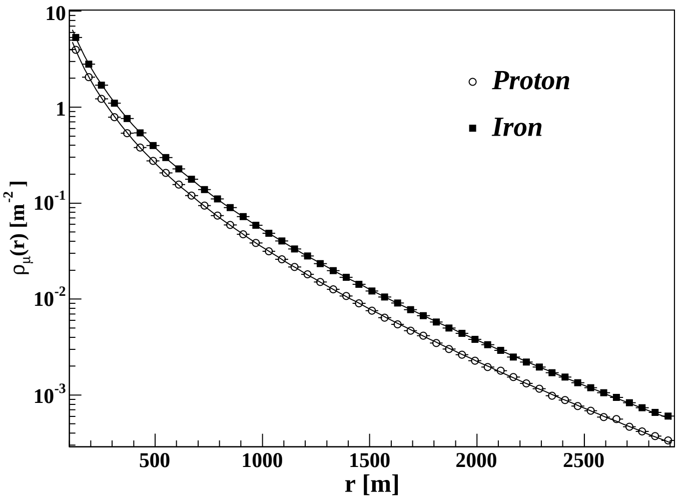

Fig. 1. Fit of the density of muons as a function of the core distance for showers of $E = 1.0EeV$ and $\theta = 30°$ initiated by iron an proton primaries.

Furthermore, the behavior of the parameter γ was analyzed using proton and iron simulations for different zenith angles ($0°, 30°$ and $45°$), taking into account the attenuation resulting from the shielding prior to reaching the muon counters. We found that γ decreases very slowly with zenith angle and is almost independent of primary composition. Therefore, as a first approximation we fixed $\gamma = 2.93$ in all subsequent analysis, leaving only P_0 and β as free fit parameters.

The Aires output is in turn used as input to the detector simulation codes. The Auger surface array response was simulated with the computer code SDSim v3r0 [6] and a modified version of it was written in order to simulate the muon counter array.

The shower reconstruction is performed by using the standard Auger reconstruction package (CDAS Erv2r4 [7]). The reconstruction of shower direction, core position and energy were obtained from the water Cherenkov detector array rather than from the muon counters. With these three parameters fixed, we proceeded to obtain the muon LDF, obtaining the results summarized in the next section.

2.3. Resolution

In order to assess the performance of a muon counter array composed of either 30 or $60m^2$ detectors, we simulated detector responses from 50 simulated showers initiated by either proton or iron of $1.0EeV$ and $45°$ of incidence angle. Each shower was used in turn to generate 20 events by randomly changing its core position within the array. We obtain the number of muons at $600m$ from the core from the fitted muon LDF. Fig. 2 shows the resolution obtained in the determination of the number of muons at $600m$ from the shower core, where we define $\epsilon(N_\mu(600)) = 1 - N_\mu^{Rec}(600)/N_\mu^{Real}(600)$ where $N_\mu^{Rec}(600)$ is the reconstructed number of muons and $N_\mu^{Real}(600)$ is the value calculated by sampling Aires muons in a $20m$ wide ring.

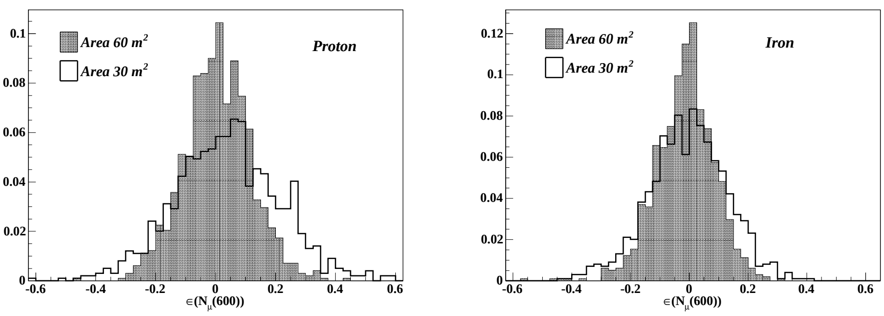

Fig. 2. Resolution in the determination of the number of muons at $600m$ from the core for proton and iron primaries and for $30m^2$ and $60m^2$ muon detectors.

The resolutions for a $30m^2$ detector were 13% and 17% for iron and proton primaries respectively, while for a $60m^2$ counter, 10% and 11%.

2.4. Abundance Determination

In order to compare the performance of the 30 and 60 m^2 muon detectors, we applied the method described in [2] to calculate the proton abundance for any given p-Fe mixture. We set off by smoothing the p and Fe histograms of the reconstructed parameter $N_\mu^{Rec}(600)$ (see Fig. 3) by assigning a gaussian distribution to each histogram point with a given width as suggested in Ref. [8] and used them as a probability distribution function, $f_A(N_\mu(600))$ with A either p or Fe.

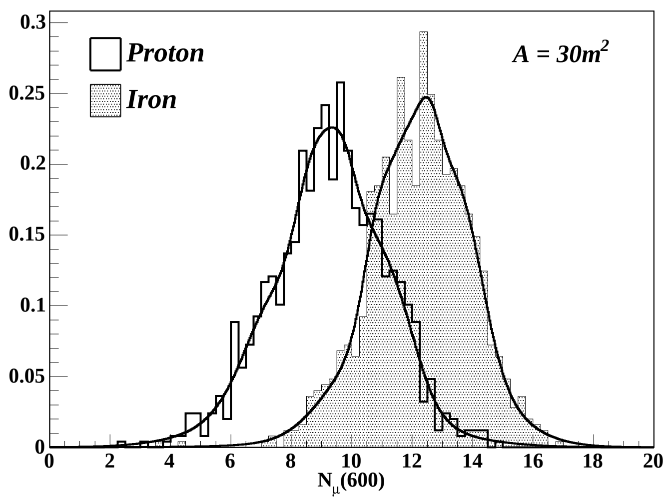

Fig. 3. Distributions of the reconstructed number of muons at 600m from the core for proton and iron primaries for assuming a 30m^2 muon counter. Also shown are the smoothed distributions used in the abundance calculation.

By using these estimated distributions we generated independent samples of 1000 events each one with compositions ranging from 0 to 100%. We calculated the proton abundance from:

$$[p]_{Ob} = \frac{1}{N} \sum_{i=1}^{N_B} N_i P(N_\mu(600)_i) \tag{3}$$

where N is the total number of events (1000), N_B is the number of bins, N_i is the number of events in $i-th$ bin, and $P(x) = f_p(x)/(f_p(x) + f_{Fe}(x))$, with $N_\mu(600)$ as defined in Eq. (2).

Figure 4 shows the obtained abundance for both 30 and 60m^2 detectors as a function of the real abundance. Note that if the muon distributions for Fe an p did not overlap, the inferred abundances should be exactly the real ones, which would be the case depicted as the shown straight line with unitary slope: a measured

$N_\mu(600)$ would suffice to identify a proton from an iron primary. On the opposite case, if the p and Fe distributions fully overlap, the inferred abundances would always be 0.5, i.e. a horizontal line irrespective of the admixture. A partial overlap, as shown in Fig. 3, yields an intermediate behavior between these extreme cases.

Fig. 4 shows that the obtained abundances have a very narrow confidence level arising from the statistical uncertainties from the considered 10000 samples of 1000 events each. Note that increasing the detector area will diminish the overlap area of the $N_\mu(600)$ p-Fe distributions due to different mean values and statistical fluctuations. This is not reflected in the band widths but rather in the line slopes, as shown in Fig. 4, which determine the size of the uncertainty when trying to infer real abundances from the observed ones.

Fig. 4 thus provides a calibration curve with a small uncertainty: for any given measured $[p]_{Ob}$, the uncertainty in the deduced $[p]_{Real}$ may be obtained by just drawing a horizontal line at $[p]_{Ob}$. This line will cross each of the two detector area bands at an entry and exit $[p]_{Real}$ values. This interval will be uncertainty in $[p]_{Real}$ (the average value can always be calibrated from the slope of the curve). From Fig. 4, the difference in uncertainty between 30 and $60m^2$ is approximately 30% and, therefore, probably the best cost to benefit ratio is obtained for the smaller detector. As a final comment it is emphasized that the disagreement between observed and real abundances will increase when further uncertainties are contemplated, in particular due to the impact on the number of muons from uncertainties in the reconstructed primary energy and from an assumption of a different hadronic model interaction [9].

3. Conclusions

In this work we proposed and studied the performance of muon density reconstructions based on reconstructed data from the Auger surface detector array, a new muon counter array computer code, and a parameterized muon LDF. Proton abundances were inferred for any given fixed p-Fe mixture for two possible values of muon detectors area at primary energies of $1.0EeV$ and a calibration curve is suggested.

We showed that the resolution in the determination of the muon number at $600m$ from the core improves with the detector area. It ranges from 13% to 17% for proton primaries and from 10% to 13% for iron primaries, when the counter area is increased from 30 to 60 m^2. This modest improvement does not seem to justify the larger detector.

References

1. Pierre Auger Collaboration, Nuc. Inst. Methods A523(2004)50; *Procs. 29th ICRC, Pune, India* (2005).
2. A. D. Supanitsky et al. *Procs. 29th ICRC, Pune, India* (2005), astro-ph/0510451.

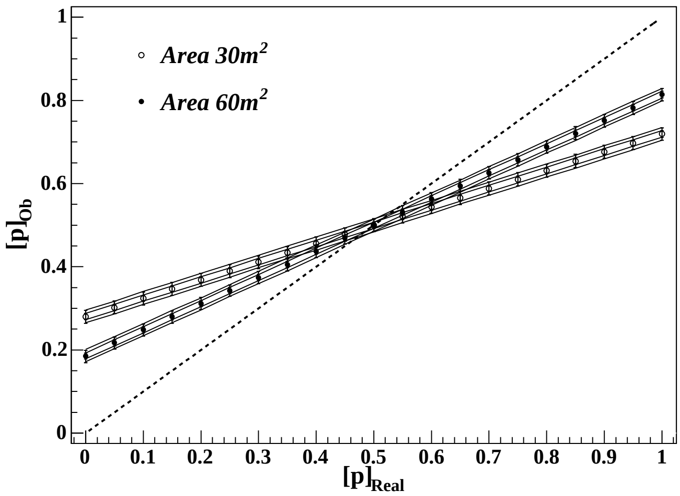

Fig. 4. Abundance obtained by applying the method outlined in the text as a function of the real abundance, the bands indicate 68% and 95% confidence levels.

3. D. Groom et al., *Atomic Data and Nuclear Data Tables* **78**
4. S. J. Sciutto, *AIRES user's Manual and Reference Guide (2002)*, http://www.fisica.unlp.edu.ar/auger/aires.
5. Andreas Haungs, personal communication.
6. http://lpnhe-auger.in2p3.fr/Silvie/WWW/AUGER/DPA
7. http://www.auger.org.ar/CDAS-Public/.
8. D. Fadda et al. *Astron. Astrophys. Suppl. Ser.* **127** (1998) 335. (2001) 183.
9. A. D. Supanitsky et al., work in progress.